Tectonic Origin Tsunami Scenario Database for the Marmara Region

Ceren Ozer Sozdinler[1], Ocal Necmioglu[2], H. Basak Bayraktar[2,3], Nurcan M. Ozel[2,4]

[1]Institute of Education, Research and Regional Cooperation for Crisis Management Shikoku, Kagawa University, Takamatsu, 760-8521, Japan

[2]Department of Geophysics, Kandilli Observatory and Earthquake Research Institute, Bogazici University, Istanbul, 34684, Turkey

[3]Department of Physics "Ettore Pancini", University of Naples Federico II, Naples, 80126, Italy

[4]International Monitoring Systems, Comprehensive Nuclear-Test-Ban Treaty Organization, Vienna, 1400, Austria

Correspondence to: Ceren Ozer Sozdinler (cerenozr@cc.kagawa-u.ac.jp)

Abstract. This study presents a tsunami scenario database in Marmara Sea, Turkey referring to 30 different earthquake scenarios obtained with the combinations of 32 possible fault segments, complemented with three additional worst-case scenarios based on catastrophic historical earthquakes. The main motivations of this study are to create a tsunami database which may assist the Regional Earthquake and Tsunami Monitoring Center (RETMC) of Kandilli Observatory and Earthquake Research Institute (KOERI) in situation assessment in case of a real event in the Marmara Sea and to investigate the nature and generation of historical tsunamis that were significantly affected Marmara region. Tsunami simulations have been performed using tsunami numerical code NAMI DANCE which solves Nonlinear Shallow Water Equations (NLSWE) using leap-frog scheme. For each earthquake scenario, tsunami hydrodynamic parameters, mainly maximum water surface elevations, arrival time of first wave and maximum wave, and time histories of water level fluctuations were calculated at 1333 synthetic gauge points meticulously selected in shallow zone offshore the coasts of Marmara Sea. Among all analyses in this study the rupture of a segment along Main Marmara Fault generates the largest tsunami source and consequently the highest wave amplitudes in the Sea of Marmara, reaching up to 2.2 m. According to the integrated maximum wave heights, the most significant effects are expected along Silivri at the north, Kursunlu, Bayramdere and Cinarcik at the south, and western Kadikoy, Princes' Islands, Maltepe and Pendik at the east. Arrival times of first waves are quite short, almost within 5 minutes for the locations close to the earthquake origin. It should be noted that, however, the maximum wave height obtained due to this deterministic study is relatively lower in comparison to the available probabilistic studies published so far. The overview of the results confirm that higher historical tsunami wave heights observed in Marmara Sea cannot be explained by only earthquake-generated tsunamis, as also indicated by recent related publications as there is strong agreement on considering submarine landslides as the primary component of tsunami hazard in the Marmara.

1 Introduction

Marmara Region is located at the northwest part of Turkey, being one of the most important settlements throughout history as the passageway between two continents, Europe and Asia. The region literally acts as the heart of economy in the country

hosting mainly the Istanbul megacity with a population of more than 15 million and huge capacity of trading and tourism, various industrial facilities, ports, airports as well as other densely populated cities.

Marmara Sea is seismically very active as part of the North Anatolian Fault Zone (NAF) with a history of large earthquakes and possibility of experiencing earthquakes with magnitudes larger than 7.0 in the future (Ambraseys, 2002). There is a large number of references in literature proving the generation of historical tsunamis in the Marmara Sea caused by these earthquakes (Mihailovic 1927; Gundogdu 1986; Oztin and Bayülke 1991; Oztin 1994; Ambraseys and Finkel, 1987, 1995; Altınok and Ersoy 2000; Arel and Kiper, 2000; Altınok et al. 2001, 2003, 2011; Yalciner et al. 2002; Ambraseys 2002; Cetin et al. 2004; Rothaus et al. 2004; Tinti et al. 2006; Özel et al. 2011). The most significant ones are the Istanbul earthquakes on 10 September 1509, on 22 May 1766, and on 10 July 1894; the Sarkoy-Murefte earthquake on 9 August 1912; and the 17 August 1999 Kocaeli earthquake (Necmioğlu, 2016). During the 1509 earthquake, with a magnitude close to 7.5 (Bulut et.al, 2019), the sea flooded the shores along Istanbul coasts, waves crashed against city walls and around 4000–5000 people died in the city (Ambraseys and Finkel 1995). Tsunami waves with probably more than 6.0 m height overtopped the city walls and caused flooding (Oztin and Bayülke 1991; Yalciner et al, 2002). 1766 Istanbul earthquake, on the other hand, triggered considerable tsunami in Besiktas, Istanbul and inner parts of Bosphorus strait, Gemlik Bay and Mudanya in Eastern Marmara (Ambraseys and Finkel 1995; Altınok et al. 2003, 2011) (The estimated origin of these earthquakes as well as observed runup values according to historical records are shown in Figure 3 in the following section).

The main motivation for this study is investigating the nature of historical tsunamis in Marmara Sea, namely whether they are generated solely due to those significant earthquakes or additional sources, such as submarine landslides triggered by the earthquakes. Due to short arrival times of first waves in Marmara coasts, having prepared tsunami scenarios covering various possible earthquakes is considered as vital, and a comprehensive tsunami database may also assist the Regional Earthquake and Tsunami Monitoring Center (RETMC) of Kandilli Observatory and Earthquake Research Institute (KOERI), an accredited Tsunami Service Provider of the Intergovernmental Coordination Group for the Tsunami Early Warning and Mitigation System in the North-eastern Atlantic, the Mediterranean and connected seas (ICG/NEAMTWS), in situation assessment complemented with real-time observations.

For this purpose, we have identified a set of credible worst-case earthquake scenarios for the whole Marmara Region obtained by the compilation of historical records, past studies in literature and empirical results. These scenarios constitute the basis for tsunami numerical modelling conducted to obtain tsunami scenario database in Marmara Sea.

2. Methodology

2.1 Identification of Earthquake Scenarios

The main structural element controlling the morphological and structural features in Marmara Sea region is the northern strand of the NAF, which is considered as a predominantly strike-slip displacement zone (Alpar and Yaltırak, 2002). The NAF, which is a major right-lateral strike-slip fault, extends more than 1200 km from eastern Turkey to the north Aegean Sea (Sengör et

al., 2005). It accommodates the relative right-lateral motion between the Anatolian region and Eurasia at a geodetic rate of ~25 mm/yr (Meade et al., 2002; Reilinger et al., 2006). Along its westernmost segment, the fault bifurcates into northern and southern branches, the northern branch following Izmit Bay and entering the Sea of Marmara southeast of Istanbul. By far the majority of long-term fault slip occurs on the northern fault branch following the northwest striking Princes' Islands Fault (PIF) and joining the east-west striking Central Marmara Fault (CMF) immediately south of Istanbul (Le Pichon et al., 2001; Armijo et al., 2005). After traversing much of the Sea of Marmara, the CMF merges with the Ganos Fault, exiting the Sea along the Ganos Peninsula. Ergintav et al. (2014) concluded that the Princes' Islands segment is most likely to generate the next M > 7 earthquake along the Sea of Marmara segment of the NAF. Armijo et al. (2005) stated that a zone of maximum loading with at least 4–5 m of slip deficit encompassing the 70 km long strike-slip segment between the Cinarcik and Central Basins would alone be capable of generating an earthquake with Mw 7.2. Hergert et al. (2011) argues that the Main Marmara Fault can be interpreted as a through-going fault that slips almost purely in a strike-slip sense, but they also point out that, not contradictory to the previous statement, there is significant dip-slip motion at some sections of the Main Marmara Fault. The South Marmara Fault lies between the highly active northern branch and the weakly active (but still capable of generating magnitude 7 earthquakes) southern branch (Le Pichon et al., 2014).

In this deterministic study, the geometry of the possible tsunamigenic faults in the Marmara Sea has been derived from the GIS Fault Database in the Marmara region produced within MARsite - New Directions in Seismic Hazard assessment through Focused Earth Observation in the Marmara Supersite (FP7 Project-ENV.2012 6.4-2, Grant 308417), as a project deliverable with restricted dissemination. Fault parameters, on the other hand, were assigned through an extensive review of the literature (Alpar and Yaltırak, 2002; Altınok and Alpar, 2006; Armijo et al., 2005; Ergintav et al., 2014; Gasperini et al., 2011; Hebert et al., 2005; Hergert et al., 2011; Hergert and Heidbach, 2010; Imren et al.; 2001; Kaneko, 2009; Le Pichon et al., 2001; Le Pichon et al., 2003; Le Pichon et al. 2014; Oglesby and Mai, 2012; Sengor et al.,2014; Tinti et al., 2006; Utkucu et al., 2009). Based on the databases and literature review, 32 faults segments were simplified in order to be able to use them as input for tsunami modelling, where each segment correspond to a rectangular area with an associated hypothetical uniform slip. The locations of each segment are given in Figure 1 where the segments lying on the same fault system (i.e. MMF, SMF, CMF, PIF) are shown in corresponding boxes. All parameters required for the identification of the segments, such as geographical coordinates for the start- and end-points of the segments, hypocentre, type of fault, strike, dip, rake, length and width of the segment, focal depth (where the top of the fault has been set to 0.5 km depth) and corresponding displacements according to empirical relations provided by Wells and Coppersmith (1994) are also presented in Table S.1. The formula provided by Wells and Coppersmith (1994) and associated parameters are given in Table 1. Standard errors defined by Wells and Coppersmith (1994) have been also considered in the Mw calculations to determine Mw (min) and Mw (max) values. Corresponding Moment values have been calculated from the $Mw = 2/3 \log M_0 - 10.7$ (Hanks and Kanamori, 1979). Corresponding displacement has been obtained from $M=\mu AD$, where A is the rupture area, D is the displacement in m and μ is the rigidity modulus taken as 3.25×10^{11} dyn/cm^2.

M=a + b x log(RA)				
Fault Type	**a**	**sa**	**b**	**sb**
Strike Slip (SS)	3.98	0.07	1.02	0.03
Reverse (R)	4.33	0.12	0.9	0.05
Normal (N)	3.93	0.23	1.02	0.1

Table 1. Empirical relations between rupture area, fault type and moment magnitude, where RA is the rupture area, a and b are the regression coefficients and sa and sb are standard error of the coefficients (Wells and Coppersmith, 1994).

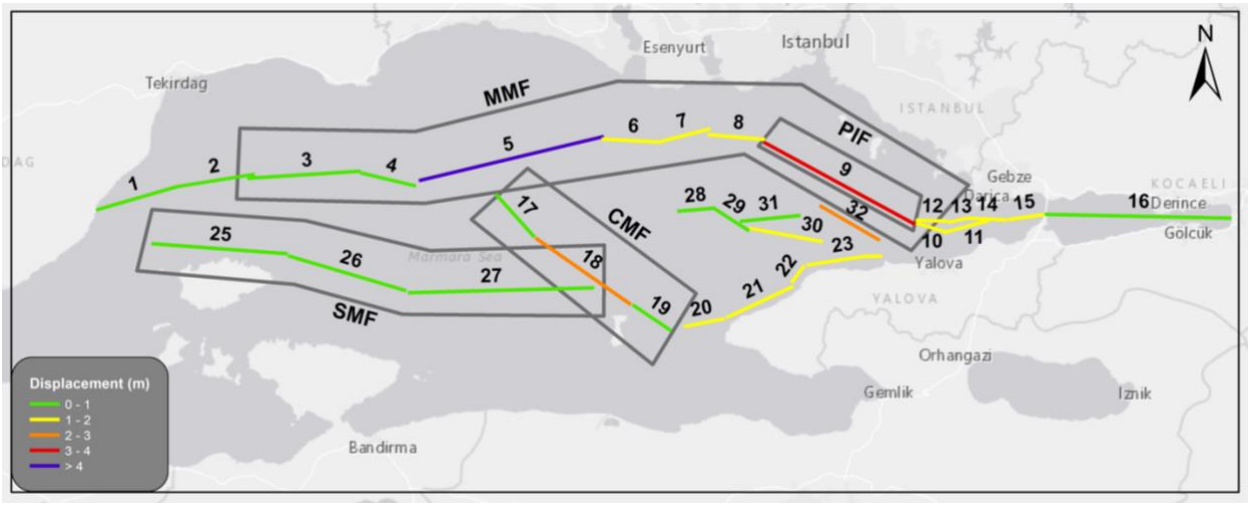

Figure 1: Simplified fault segments in Marmara identified for tsunami modelling. Fault lineaments are simplified from GIS Fault Database in the Marmara region produced within MARsite Project. The segments located in the same fault system are shown in grey-lined boxes (MMF: Main Marmara Fault, PIF: Princes' Islands Fault, SMF: South Marmara Fault, CMF: Central Marmara Fault). Segments correspond to a rectangular area with an associated uniform slip, i.e. the slip is uniform for each segment, but varies from one segment to another. The main characteristics of the plotted fault segments are summarized, and corresponding slip values are given in Table S.1 in the Supplement Material.

This was followed by the definition of different hypothetical rupture scenarios reaching a total number of 30 scenarios. The total earthquake moment for each scenario is derived from the summation of the moments associated to the individual segments considered to be ruptured in a given scenario. Slip values have been assigned randomly without any prior assumption, so that heterogeneous earthquake rupture scenarios can be represented. It should be noted, that while the individual segments are assigned with a homogeneous slip, scenarios (except SN06 and SN25) are composed of a combination of segments which represents a heterogeneous slip distribution to the extent possible. These 30 earthquake scenarios derived by this approach are shown in Figure 2 and the details of each scenario in terms of slip values and moment magnitudes are described in Table S.2 in Supplementary Material.

It is arguable that the maximum earthquake scenarios with Mw 7.4 obtained by Wells and Coppersmith (1994) in this study may not represent all possible significant earthquakes in the region. In their recent publication, Murru et al. (2016) combined a total of 10 different Mw = 7.0 to Mw = 8.0 multi-segment ruptures with the other regional faults at rates that balance the overall moment accumulation and they found an aggregated 30-year Poisson probability of M > 7.3 earthquakes at Istanbul of 35%, which increases to 47% if time dependence and stress transfer are considered. They indicated that considering the stress transfer effect from the Izmit earthquake in the calculations, the combined probability to have an event with M ≥ 7.0 up to M8.0 at Istanbul city becomes 47%. Bulut et al. (2019) reported that the present-day slip deficits reach up to 1.7 m beneath the Western (Tekirdağ Basin) segment, and 4.0 m and 5.4 m beneath the Central (Central High and Kumburgaz Basin) and Eastern (Çınarcık Basin) segments, respectively. These segments most recently ruptured in August 1766, May 1766 and October 1509 and currently have a potential to generate Mw 7.2, Mw 7.4 and Mw 7.5, earthquakes respectively. Although contiguous ruptures have not occurred historically, ruptures of contiguous segments could occur as a Mw 7.5 earthquake in the west, or a Mw 7.6 earthquake in the east or as a single through-going Mw 7.7 rupture. In consequence of these evaluations, alongside 30 earthquake scenarios, we also performed tsunami simulations for three historical big earthquakes, Mw 7.5 1509, Mw 7.3 May 1766 and Mw 7.4 August 1766 earthquakes, as complement worst-case scenarios proposed by Bulut et al (2019). Associated slip values for these earthquakes have been derived from Hanks and Kanamori (1979), considering the fault length (L), fault width (W), Mw (Bulut et al., 2019) and rigidity modulus (3.25×10^{11} dyn/cm^2), as shown in Table 2. It's noteworthy, however, that the empirical relationships proposed by Wells and Coppersmith (1994) results with lower Mw and associated slip values for these earthquakes (shown as WC94 in Table 2). The reason for that is mainly due to the fact that Mw values proposed by Bulut et al. (2019) are based on a mean slip deficit rate of 9.9 mm/year derived from a summation of the seismic moment released by historical earthquakes for a period of 1500 years.

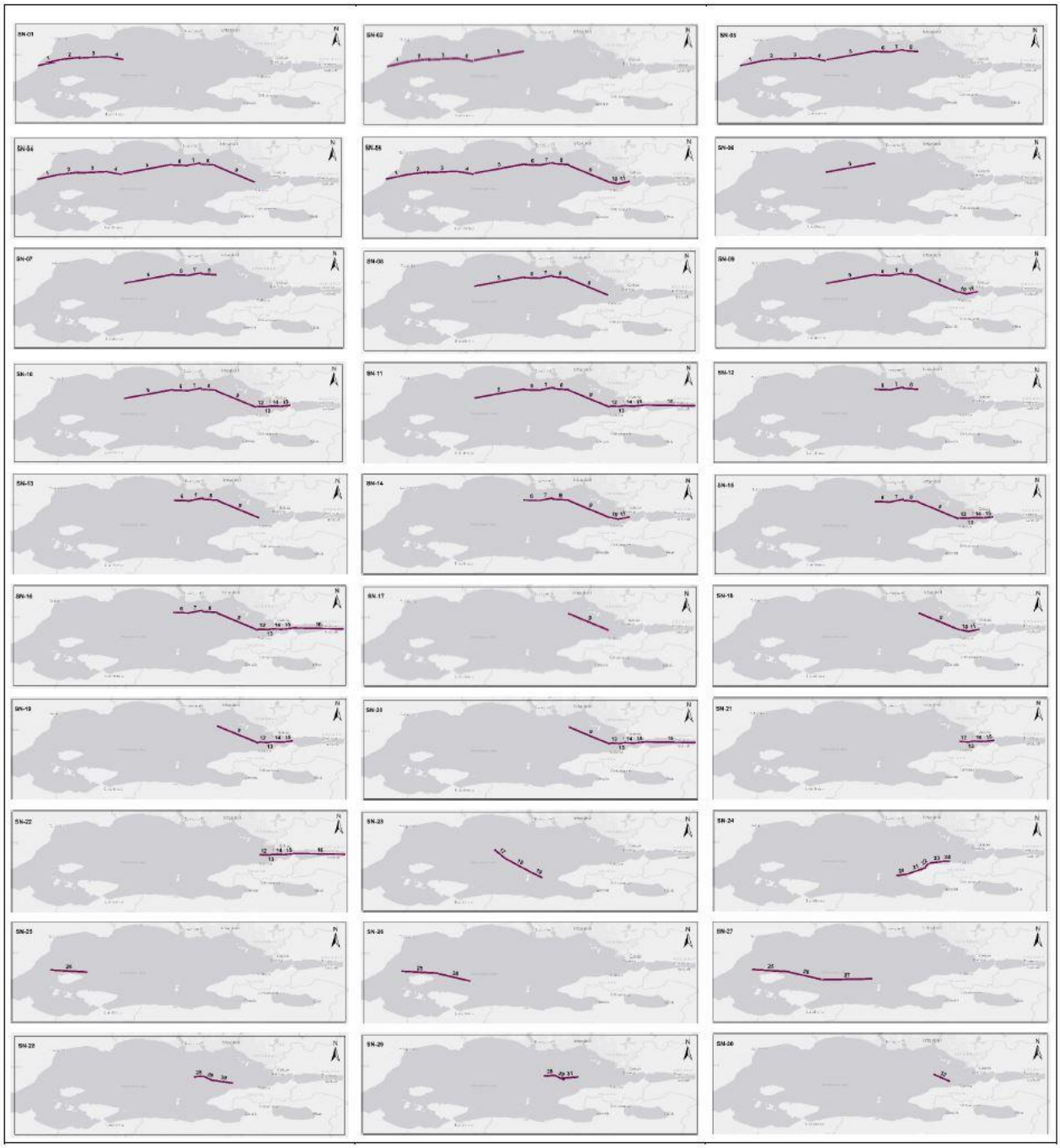

Figure 2: Map representation of the scenarios considered in this study. The details of each scenario in terms of corresponding slip values and moment magnitudes are described in Table S.2 in Supplementary Material.

Year	Mw (Bulut 2016)	Segments	Total RA	L	W	D(m)*	Mw(WC94)	D(m) (WC94)
1509	7,5	6,7,8,9	1310	66	20	5,2	7,3	2,6
1766a	7,3	4,5	950	48	20	3,5	7,2	2,5
1766b	7,4	2,3,4	720	48	20	5,1	7,2	2,5
**** same in each segment***								

Table 2: Fault parameters assigned in this study for three historical big earthquakes, Mw 7.5 1509, Mw 7.3 May 1766 and Mw 7.4 August 1766 earthquakes, as complement worst-case scenarios proposed by Bulut et al (2019).

2.2 Tsunami Numerical Modeling of 30 earthquake scenarios

Tsunami numerical modeling has been performed based on 30 earthquake scenarios defined in Section 2.1 using the numerical code NAMI DANCE (NAMIDANCE, 2011). NAMIDANCE solves Nonlinear Shallow Water Equations (NLSWE) with leap-frog scheme both in Cartesian and Spherical coordinate system, which was tested, validated and verified against analytical solutions, laboratory measurements and field observations in several scientific articles (NTHMP, 2017; Lynett et al., 2017; Velioğlu, 2017; Ozer Sozdinler et al, 2015).

Tsunami numerical modelling is performed using 90m grid sized bathymetry - topography data as a single study domain. It was prepared by compiling various data as multi-beam bathymetric measurements, 900m grid sized GEBCO data in the sea as well as 30m grid sized ASTER data on land. Besides, coastline and coastal defence structures i.e. breakwaters, groins and large docks in the ports were also digitized in GIS environment and added to bathymetry - topography data for increasing the resolution and precision in coastal zones. Higher-resolution ASTER data has an important role in data compilation process as it is denser compared with the bathymetry data. In that way, interpolation between less sensitive bathymetry data and much denser topography data provides more reliable coastline in 90m grid sized study domain. The precision in coastline supports the process of selecting synthetic gauge points in shallow zone very close to shoreline, which is described in coming sections below.

The initial sea surface at the time of fault rupture for each segment has been calculated using Okada (1985) formula. In each scenario, it was assumed that all designated fault segments are ruptured simultaneously. NAMIDANCE calculates the sea surface after the rupture of each segment and combines each calculation to output the resultant sea surface as the tsunami source of each scenario. For instance, for Earthquake Scenario #1 (SN01), segment-1, segment-2, segment-3 and segment-4 are the designated fault components for this scenario. The sea surface for each fault segment is calculated using Okada (1985) formula. NAMIDANCE then outputs a resultant sea surface as the combination of these simultaneously ruptured four segments as an overall tsunami source for SN01. We applied the same procedure for all earthquake scenarios accordingly. The maximum and minimum water surface elevations corresponding to the tsunami initial condition computed for each scenario are given in Table S.3 in Supplementary Material. As seen from the table, the initial sea surface disturbances for all scenarios are less than 1 m. The highest sea surface was calculated for SN23, which includes the rupture of segments 17, 18 and 19 located at the center of Marmara Sea striking in NW-SE direction.

The synthetic gauge points along the coasts of Marmara Sea were first selected with very sensitive analysis so as to locate them in shallow zone at water depths less than 50 m. We basically considered the locations of industrial facilities, residential areas, harbors, marinas, factories and six Tsunami Forecast Points (TFPs) while selecting those gauge points (TFPs are synthetic gauge points located at Marmara Eregli, Haydarpasa, Yalova, Mudanya, Erdek and Degirmencik, where the arrival time of first wave and tsunami alert level are calculated and included in national tsunami alert messages disseminated from Regional Tsunami and Earthquake Monitoring Center in KOERI; see Figure 3. There are additional 42 TFPs along the coasts of Turkey in Black Sea, Aegean Sea and Mediterranean Sea). After the selection of synthetic gauge points, test runs were performed in order to identify the water depth where NAMIDANCE located each gauge point as the software assigns each synthetic point at the nearest grid node in bathymetric and topographic data. In other words, although gauge points were selected in the sea within the shallow zone less than 50 m water depth they may be relocated on land or at locations deeper than expected due to the input principles of NAMIDANCE. For that reason, test analyses are critical to validate that synthetic gauge points are located in shallow zone at the possible shallowest location. After these validation analyses, the total number of 1333 gauge points were defined, most of which were located at the water depths of less than 10 m (water depths at some of the gauge points are higher than 10m due to steep topographic conditions at some regions). It is noted that the northern part of the area has much more critical locations than the southern part; therefore, gauge points in that region are denser than the southern part of the Marmara.

Tsunami simulations were conducted for each scenario for 2 hours using the corresponding tsunami sources. The simulation time used for 30 earthquake scenarios was defined after trial simulations performed for the selection of synthetic gauge points as described previously above. As a result of these analyses, it was decided as 2 hours wave propagation in the Sea of Marmara would be adequate to obtain maximum wave amplitudes as well as arrival time of first waves at gauge points. The water level fluctuation was still observed after 2 hours; however, the wave heights were not so significant and less than the maximum values. It should be also noted that such wave motion was observed mostly at the gauge points located in enclosed basins where wave reflections are significant.

Tsunami hydrodynamic parameters as maximum and minimum wave amplitudes, arrival times of first and maximum wave, flow depths and current velocities were calculated throughout Marmara basin and at 1333 synthetic gauge points. We discuss the simulation results in the following section in an integrated manner instead of giving the details of each scenario results in the main text of this paper. Instead, the distributions of maximum wave amplitudes and arrival time of first wave plotted for each scenario are provided in Supplementary Material. These plots directly reflect the hydrodynamic parameters calculated at each synthetic gauge point according to the defined color scale. In addition, Supplementary Material also includes water level fluctuations calculated for each scenario at six TFPs (Haydarpasa, Yalova, Mudanya, Erdek, Degirmencik and M. Eregli) and also 20 other locations that are selected out of 1333 synthetic gauge points considering the locations of industrial facilities, harbors, marinas, refineries and shipyards. These fluctuation plots also indicate the arrival time of first wave at each location. The maximum wave amplitudes less than 75 cm were coloured with green as a representative of relatively safer coastal zones of Marmara Sea. Several experimental and numerical studies in literature prove that 30 cm inundation depth can be accepted

as threshold for critical water level that has potential to cause a person to fall down (Jonkman and Penning-Rowsell, 2008; Takagi et al., 2016). So, according to the distribution and relation between the maximum wave amplitudes calculated at gauge points in the sea and inundation depth values calculated on land, the value of 75 cm wave amplitude was decided as to define relatively safer coastal zones.

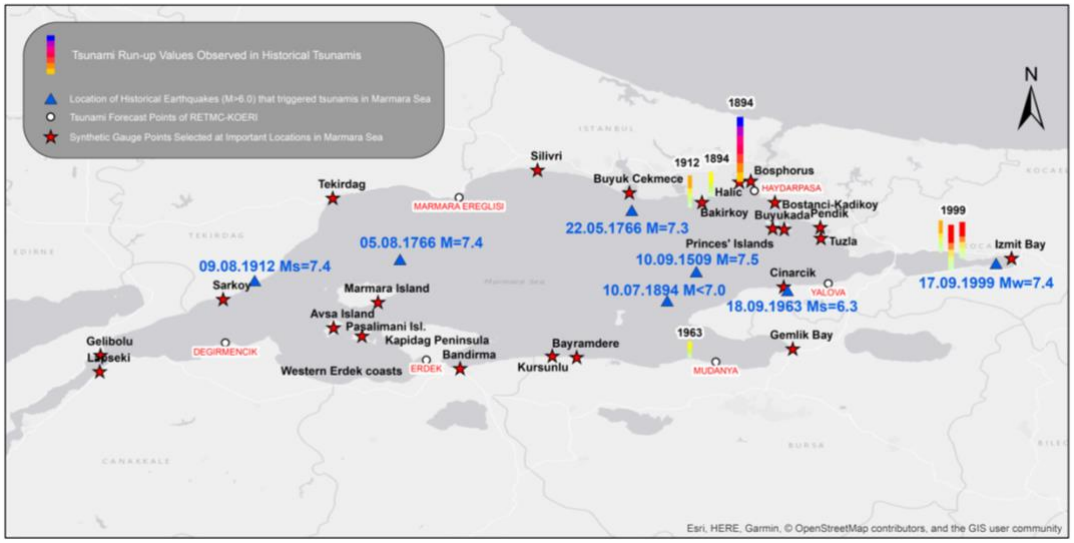

Figure 3: The locations of Tsunami Forecast Points (white dots and white-highlighted names written in red) and other important coastal districts (red stars and names written in black) where estimated tsunami effect is significant. The origin of historical earthquakes with M>6.0 are also located referring to Altinok et al (2011) and Bulut et al (2019). For the 1509 and 1766 earthquakes, proposed epicentres in these studies differ significantly and preference was given to Bulut et al. (2019). The bar charts show the tsunami runups observed after the earthquakes written on top of each bar (source: Altinok et al, 2011). The color scale of bar chart is 0-1 m: green, 1-2 m: yellow, 2-3 m: orange, 3-4 m: red, 4-5 m: purple.

2.2.1 Summary of Results

As described in previous section, the simulation results are presented here as an integrated distribution of maximum wave amplitudes for overall tsunami scenario database in Marmara Sea. The maximum wave amplitudes were calculated at each synthetic gauge point for 30 earthquake scenarios. The calculated results of 30 scenarios at each gauge point were sorted from higher to smaller and the highest value was stored as the representative maximum wave amplitude at this gauge point. After defining all maximum wave amplitude values at 1333 synthetic gauge points, their integrated distribution was plotted for the entire Marmara Sea (Figure 4). As described in previous section, the coastal zones with green color represents relatively safer locations according to the earthquake scenarios in this database.

Following the same procedure, the integrated distribution of arrival time of maximum waves (that is the time of occurrence of maximum wave amplitude at each gauge point in entire earthquake scenarios) was plotted in Figure 5. The results show that the arrival of maximum waves is expected at Princes' Islands, Yalova coasts, some parts of Kadikoy and Silivri coasts within 5 minutes, which is critically short time for evacuation (refer to Figure 3 for the locations of affected districts).

Summary of the simulation results are given in Table 3 including the calculated maximum wave amplitudes for corresponding earthquake scenario and the names of most affected coastal regions. The results show that the highest wave heights are estimated offshore southern coasts of Marmara Sea (Bayramdere and Kursunlu; coastal towns of Bursa city) as 2.2m due to SN06. Other significantly affected locations are Western Kadikoy (Kalamis) and Silivri coasts with maximum wave heights between 1.75 m and 2 m. The estimated maximum wave heights for Princes' Islands, northern entrance of Bosphorus (Halic, Fatih); Bakirkoy, B. Cekmece; Pendik, Maltepe and Cinarcik (Esenkoy) are between 1.25 m and 1.5 m. Wave heights reach up to 1.25 m at M. Eregli, Zeytinburnu, Tuzla and Yalova and 1 m at Haydarpasa, Uskudar, entrance of Izmit and Gemlik Bays, Kapidag Peninsula, Marmara Island and Bandirma, respectively. The lowest wave heights are calculated around Gelibolu and Lapseki (Canakkale city), southern and western Marmara Island; Avsa and Pasalimani Islands; innermost locations of Izmit and Gemlik Bays, northern Bosphorus, western Kapidag Peninsula, western Erdek coasts, Sarkoy coasts and Tekirdag. It is once again noted that simulation results are evaluated according to the maximum wave amplitudes in shallow zone calculated at synthetic gauge points.

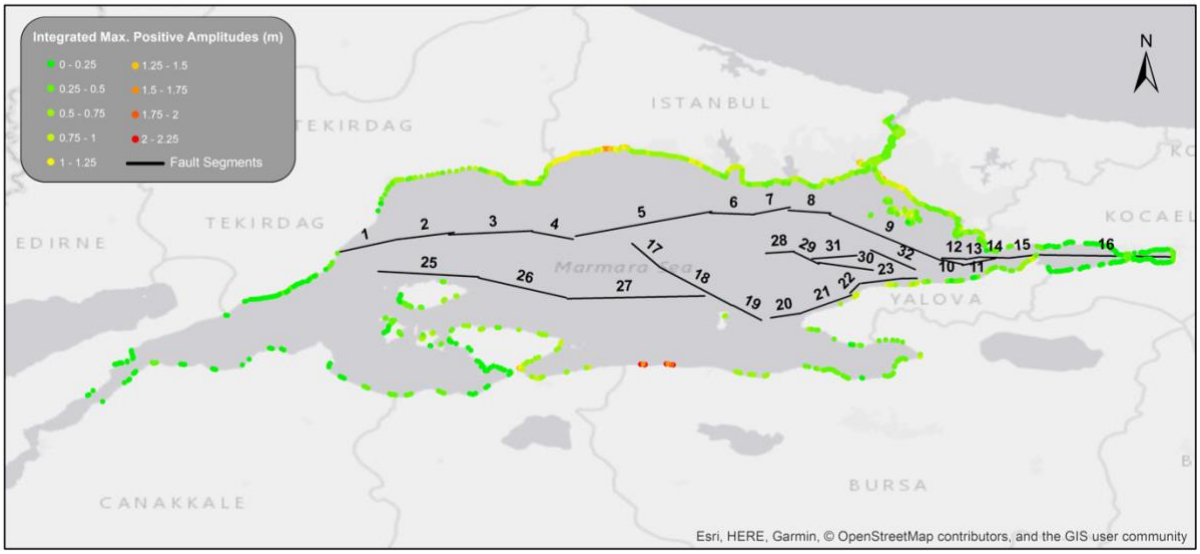

Figure 4: The integrated distribution of maximum wave amplitudes calculated at each gauge points for 30 earthquake scenarios. The fault segments used in the scenarios are also plotted in black lines.

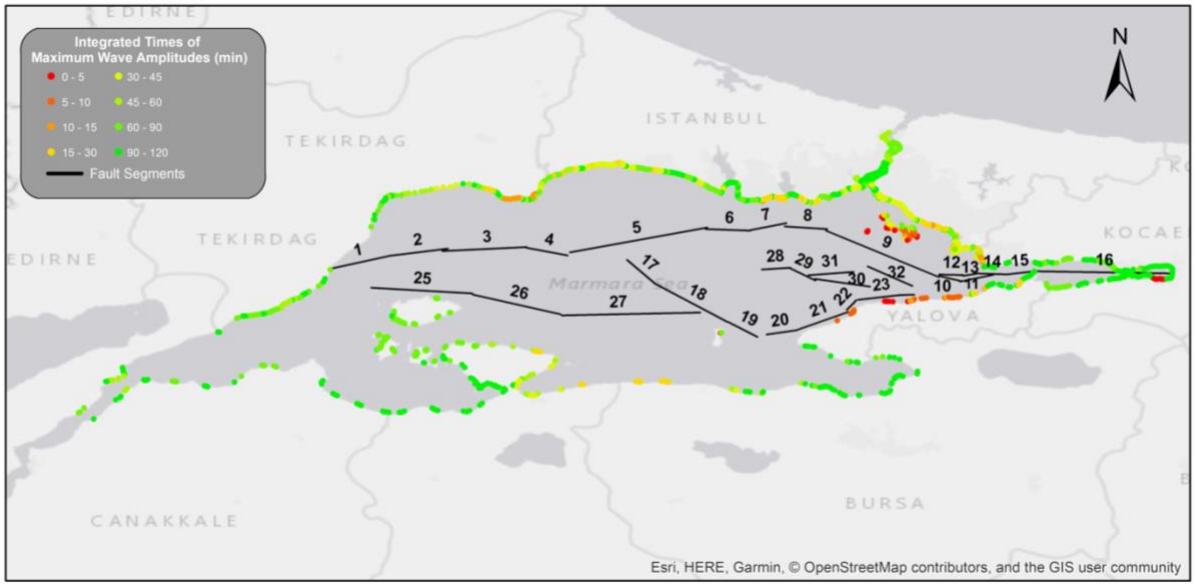

Figure 5: The integrated distribution of arrival times of maximum wave amplitudes calculated at each gauge points for 30 earthquake scenarios. The fault segments used in the scenarios are also plotted in black lines.

Maximum calculated wave amplitude	Corresponding scenario	Name of mostly affected coastal region
>2m	SN06	Kursunlu, Bayramdere (southern Marmara coasts)
1.75m – 2m	SN02, SN03, SN07, SN08, SN09, SN23	Western Kadikoy (Kalamis), Bayramdere, Silivri coasts
1.5m – 1.75m	SN04, SN05, SN10	Silivri coasts, Kadikoy district, Kursunlu, Bayramdere
1.25m – 1.5m	SN11, SN13, SN15, SN17, SN18, SN19, SN30	Princes' Islands (Buyukada), Kadikoy, Halic, Fatih, Bakirkoy, B. Cekmece, Pendik, Maltepe, Cinarcik (Esenkoy)
1m – 1.25m	SN14	Yalova, Western Silivri coasts, M. Eregli, Tuzla, Pendik, Cinarcik, Zeytinburnu
0.75m – 1m	SN16, SN20, SN29	Entrance of Izmit and Gemlik Bays, Kapidag Peninsula, Marmara Island, Haydarpasa, Uskudar, Kadikoy, Fatih, Tuzla, Maltepe, Princes' Islands (Heybeliada, Burgazada, Buyukada), Bandirma, Cinarcik
Negligible effect	SN01, SN12, SN21, SN22, SN24, SN25, SN26, SN27, SN28	Gelibolu, Lapseki, Degirmencik; Southern and Western Marmara Island; Avsa and Pasalimani Islands; innermost locations of Izmit and Gemlik Bays, northern Bosphorus, western Kapidag Peninsula, Sarkoy coasts, Tekirdag

Table 3: The calculated maximum wave amplitudes with corresponding scenarios and the names of most affected coastal regions in Marmara Sea (the locations of affected coastal regions are shown on the map in Figure 3).

2.3. Simulation of 1509, May 1766 and August 1766 earthquakes

Three catastrophic historical earthquakes, one in 1509 and two in 1766 (Bulut et al, 2019), were simulated as additional credible worst-case scenarios referring to input data given in Table 2. The earthquake of 10 September 1509 Mw 7.5 is similar to scenario SN13, whereas earthquakes of 22 May 1766 Mw 7.3 (1766a) and 5 August 1766 Mw 7.4 (1766b) are close to scenarios SN4 and SN1, respectively, but with considerably higher slip values as described in earlier sections. The simulation time for the analyses of these historical earthquakes were used as 4 hours this time to observe the change of tsunami hydrodynamic parameters in longer wave propagation as the slip values here are much higher than previously simulated 30 scenarios. Maximum and minimum initial water surface elevations of tsunami sources for these three scenarios are given in Supplementary Material (Table S.4).

Similar with the previous analyses, the simulation results of these three scenarios, 1509, 1766a and 1766b, are given in Supplementary Material as distribution of maximum wave amplitudes and arrival time of first wave along the coasts of Marmara Sea and also water level fluctuations calculated at TFPs and 20 other important locations. The results show that 1509 earthquake has higher effects along the coasts among these historical earthquakes. The mostly affected coasts due to 1509 earthquake were estimated as Kadikoy, Maltepe, Princes' Islands at the north and Cinarcik, Bayramdere and Kursunlu at the south with the wave heights between 1.5 m and 2 m. Water level fluctuations calculated for 1509 earthquake at each TFP are also relatively higher than other scenarios (see Supplementary Material Figure S.122). The southern entrance of Bosphorus, Halic, Bakirkoy, Zeytinburnu, Tuzla and Pendik coasts, and also the entrance of Izmit Bay is expecting to have significant wave heights between 1 m and 1.5 m. First waves are arriving to B. Cekmece, Bakirkoy, Halic, Bosphorus, the entire Kadikoy coasts, Tuzla, Pendik, Princes' Islands, Izmit Bay except innermost locations, Yalova, Cinarcik, Gemlik Bay and Mudanya within 5 minutes. Therefore, these locations are said to be critical in terms of tsunami early warning and evacuation. For May 1766 earthquake (1766a) significant wave heights are calculated at Silivri coasts at the north and Bayramdere and Kursunlu at the south between 1m and 1.7 m. Northern Marmara coasts, as B. Cekmece, Silivri and M. Eregli coasts are also affected from the waves with the heights up to 1 m. The effects due to 1766a earthquake are not significant along Tekirdag, Canakkale (Gelibolu, Lapseki), Marmara and Avsa Islands, Kapidag Peninsula, Bandirma and innermost locations of Izmit and Gemlik Bays. Arrival of first waves are expected within 5 minutes along M. Eregli, Silivri, B. Cekmece, Cinarcik, Avsa and Marmara Islands, Bandirma, Kursunlu and Bayramdere coasts. The effects are shifted westward for August 1766 earthquake (1766b) obviously due to the rupture location. The lowest wave heights were calculated for 1766b earthquake among these historical earthquakes. The highest wave heights occurred at northern Marmara coasts in M. Eregli and Silivri, and northern Kapidag Peninsula with the wave heights up to 1.1 m. Some locations at western Tekirdag, northern Marmara and Pasalimani Islands

are also affected. Wave heights are not so significant at the remaining locations such as Canakkale, Sarkoy, Avsa Island, western Erdek coasts, Istanbul, Izmit and Gemlik Bays. The summary of the results are given in Table 4.

Maximum wave amplitude calculated	Corresponding scenario	Name of most affected coastal region
>2m	1509	Western Kadikoy
1.75m – 2m	1509	Kadikoy, Cinarcik (Esenkoy)
1.5m – 1.75m	1509, 1766a	Kadikoy, Cinarcik, Bayramdere, Princes' Islands (Buyukada, Heybeliada), Maltepe, Kursunlu
1.25m – 1.5m	1509, 1766a	Fatih, Kadikoy, Halic, Bakirkoy, Silivri, Bayramdere, Pendik, Maltepe, Kursunlu
1m – 1.25m	1509, 1766a, 1766b	Kadikoy, Maltepe, Pendik, Tuzla, Princes' Islands, Zeytinburnu, Bakirkoy, Silivri, M. Eregli Cinarcik, Kapidag Peninsula
0.75m – 1m	all	M. Eregli, Fatih, Halic, Princes' Islands
<0.75m	all	Beylikduzu, Bandirma, Kartal, inner locations of Izmit and Gemlik Bays, Yalova, Northern Bosphorus, Tekirdag, Avsa Island

Table 4: The calculated maximum wave amplitudes with corresponding historical earthquake scenarios and the names of most affected coastal regions in Marmara Sea (the locations of affected coastal regions are shown on the map in Figure 3).

3. Discussion

This study presents a deterministic tsunami scenario database, based on 30 different earthquake scenarios obtained with the combinations of 32 possible fault segments, complemented with three additional credible worst-case scenarios based on historical earthquakes occurred in 1509, May 1766 and August 1766 referring to Bulut et al. (2019). The results of this deterministic scenario database were presented as arrival times of first and maximum waves, maximum wave heights along Marmara coasts as well as integrated maps, water level fluctuations at selected tsunami forecast points and critical important locations in the Marmara Sea. The overall simulation results reveal that the maximum wave height calculated in sensitively selected synthetic gauge points in shallow zone within entire tsunami scenario database does not exceed 2.2 m. Among all scenarios, SN06 (rupturing of Segment-5 located along Main Marmara Fault) generates the largest tsunami source and

consequently the highest wave amplitudes in the Sea of Marmara. The highest wave amplitude calculated among three historical earthquake scenarios is 2 m for 1509 earthquake. However, this value is quite lower than the historical wave records (more than 6.0 m wave height overtopped the city walls and caused flooding (Oztin and Bayülke 1991; Yalciner et al, 2002)). This outcome shows that higher historical tsunami wave heights observed in Marmara Sea cannot be explained by only earthquake generated tsunamis. Submarine landslides should be inevitably considered as the primary tsunami hazard component in the Marmara Sea. As proved by several previous studies, possible tsunamis from submarine landslides in the Marmara Sea could be significantly higher than those from earthquakes depending on the landslide volume. In addition, waveforms from all the coasts around the Marmara Sea indicate that other coastal residential areas in the Marmara region might be subject to high risk of tsunami hazards from submarine landslides, which can generate higher tsunami amplitudes and shorter arrival times, compared to Istanbul (Latcharote et al., 2016). Latcharote et al (2016) argued that the maximum tsunami height could reach 4.0 m along Istanbul shores for a full submarine rupture of the NAF, with a fault slip of 5.0 m in the eastern and western basins of the Marmara Sea, which would correspond to an earthquake with Mw 7.6. However, the maximum tsunami height for landslide-generated tsunamis from small, medium, and large of initial landslide volumes (0.15, 0.6, and 1.5 km3, respectively) could reach 3.5, 6.0, and 8.0 m, respectively, along Istanbul shores and therefore possible tsunamis from submarine landslides could be significantly higher than those from earthquakes, depending on the landslide volume significantly.

Moreover it should be noted, however, that the maximum wave height calculated in this study is relatively lower in comparison to the available probabilistic studies published so far, such as Hancilar (2012), which provide inundation maps resulting from probabilistic tsunami hazard analysis for a 10% probability of exceedance in 50 yr including the building numbers and types, lifeline systems and demographic data in Istanbul, reaching run-up height of 5-6 m. Hancilar (2012) also highlights that the residential buildings at risk are mainly located in Kadikoy, Tuzla, Bakirkoy and Princes' Islands where our study points out significant wave heights as well.

As indicated earlier, slip values for the scenarios considered in this study has been assigned randomly, reaching to a maximum of 4.5 m on the Main Marmara Fault, but comparable to the slip values used in many previous studies. Latcharote et al. (2016) proposes that the Mw 7.2 eastern rupture, the Mw 7.5 western rupture, and the Mw 7.6 full rupture scenarios considered by Hebert et al. (2005) generated a mean displacement on the fault of 4.3, 4.0, and 4.1 m, respectively. Tinti et al. (2006) suggested the generating mechanisms of the 1999 Izmit bay tsunami, in which the Marmara fault in the eastern rupture had the slip of 1.0 m. Oglesby and Mai (2012) suggested the fault geometry and stress parameters along the NAF, including the final slip patterns of less than 3.5 m. Ergintav et al. (2014) suggested the slip deficits accumulated, since the last major earthquake which is less than 2.0 m for the western rupture and 3.7 m for the eastern rupture. Last but not least, Armijo et al. (2005) suggested that the 1912 rupture appears to have crossed the Ganos restraining and bend into the Sea of Marmara floor for 60 km with a right-lateral slip of 5.0 m and Coulomb-stress modeling shows a zone of maximum loading with at least 4.0–5.0 m of slip deficit along the strike–slip segment 70 km between the Cinarcik and Central Basins. The slip values considered in this study are in compliance with these studies.

It should be also noted that the recent literature addresses the possibility of a tsunami within a strike-slip fault system due to direct earthquake-induced uplift and subsidence, as it was the case in Palu Bay after the September 2018, Mw 7.5 Sulawesi earthquake (Ulrich, et al. 2019). Nevertheless, as also indicated by Goda et al. (2019), there are mixed opinions in the current literature, with regard to the devastating tsunami damage caused by this earthquake, and the possibility of landslide component cannot be excluded (Heidarzadeh et al, 2019; Pakoksung et al, 2019; Mikami et al., 2019; Yolsal-Çevikbilen and Taymaz, 2019). Future sensitivity studies complemented with probabilistic methods considering these phenomena could definitely provide a better insight to tsunami hazard and risk in the Marmara region.

The tsunami database considered in this study addresses only possible earthquake generated tsunamis and calculated maximum wave height does not reach the level of the values historically observed. This outcome points out that a tsunami warning system for the Marmara region should be decoupled from the earthquake parameters. To address this issue, Necmioglu (2016) proposed a tsunami warning system in the Marmara region coupled with the existing earthquake early warning system, which could work without waiting for any focal mechanism parameter determination that may lead to underestimate tsunami hazards in the case of a strike–slip fault earthquake, due to the fact that submarine landslides could generate large tsunamis in the Marmara Sea.

Acknowledgements

This work is supported by MARsite - New Directions in Seismic Hazard assessment through Focused Earth Observation in the Marmara Supersite (FP7 Project-ENV.2012 6.4-2, Grant 308417). We would like to thank Cengiz Zabcı (Istanbul Technical University) and Pierre Henry, Julia Kende, Celine Grall (Centre Européen de Recherche et D'enseignement des Géosciences de L'environnement-CEREGE) for their study on "GIS database of the fault parameters" within MARSite. We would also like to acknowledge Earthquake and Tsunami Disaster Mitigation in the Marmara Region and Disaster Education in Turkey (MARDiM) Project supported by Japan International Cooperation Agency (JICA). The maps in this paper were created using ArcGIS® software by Esri. ArcGIS® and ArcMap™ are the intellectual property of Esri and are used herein under license. Copyright © Esri. All rights reserved. For more information about Esri® software, please visit www.esri.com.

References

Alpar, B. and Yaltırak, C.: Characteristic features of the North Anatolian Fault in the eastern Marmara region and its tectonic evolution, Marine Geology 190, 329-350, 2002.

Altınok, Y., Alpar, B., Özer, N. and Aykurt, H.: Revision of the tsunami catalogue affecting Turkish coasts and surrounding regions, Natural Hazards Earth System Science, 11, 273–293, 2011.

Altınok, Y. and Alpar, B.: Marmara Island earthquakes, of 1265 and 1935; Turkey, Nat. Hazards Earth Syst. Sci., 6, 999–1006, 2006.

Altınok, Y., Alpar, B. and Yaltirak, C.: Sarkoy-Murefte 1912 Earthquake's Tsunami, extension of the associated faulting in the Marmara Sea, Turkey, J Seismol., 7, 329–346, 2003.

Altınok, Y. and Ersoy, S.: Tsunamis observed on and near the Turkish coasts, Natural Hazards, 21, 185–205, 2000.

Altınok, Y., Tinti, S., Alpar, B., Yalçıner, A. C., Ersoy, S., Bortolucci, E. and Armigliato, A.: The tsunami of August 17, 1999 in Izmit Bay, Turkey, Nat Hazards, 24, 133–146, 2001.

Ambraseys, N.: The seismic activity of the Marmara Sea region over the last 2000 years, Bulletin of the Seismological Society of America, 92, 1, 1-18, 2002.

Ambraseys N. N. and Finkel, C.: The seismicity of Turkey and adjacent areas. A historical review, 1500–1800, Eren Yayıncılık, 1995.

Ambraseys N. N. and Finkel, C.: The saros–marmara earthquake of 9 August 1912, Earthquake Engineering Structural Dynamics, https://doi.org/10.1002/eqe.4290150204, V15, Issue2, 189-211, 1987.

Arel, E., Kiper, B.: The coastal landslide occurred by August 17, 1999 earthquake at Degirmendere (Kocaeli). Proceedings of Coastal Engineering 3rd National Symposium, October 5–7, 2000. Canakkale,Turkey, pp 45–55 (in Turkish), 2000.

Armijo, R., Pondard, N., Meyer, B., Uçarkus, G., Mercier de Lépinay, B., Malavieille, J., Dominguez, S., Gustcher, M-A., Schmidt, S., Beck, C., Çagatay, N., Çakir, Z., Imren, C., Eris, K., Natalin, B., Özalaybey, S., Tolun, L., Lefèvre, I., Seeber, L., Gasperini, L., Rangin, C., Emre, O., and Sarikavak, K.: Submarine fault scarps in the Sea of Marmara pull-apart (North Anatolian Fault): Implications for seismic hazard in Istanbul, Geochem. Geophys. Geosyst., 6, Q06009, doi:10.1029/2004GC000896, 2005.

Bulut, F., Aktuğ, B., Yaltırak, C., Doğru, A. and Özener, H.: Magnitudes of future large earthquakes near Istanbul quantified from 1500 years of historical earthquakes, present-day microseismicity and GPS slip rates, Tectonophysics 764,77–87, 2019.

Cetin, K.O., Isik, N., Unutmaz, B.: Seismically induced landslide at Degirmendere Nose, Izmit Bay during Kocaeli (Izmit)-Turkey earthquake. Soil Dyn Earthqu Eng 24:189–197, 2004.

Ergintav, S., Reilinger, R. E., Çakmak, R., Floyd, M., Çakır, Z., Dogan, U., King, R. W., McClusky, S., and Özener, H.: Istanbul's earthquake hot spots: Geodetic constraints on strain accumulation along faults in the Marmara seismic gap, Geophys. Res. Lett., 41, doi:10.1002/2014GL060985, 2014.

Gasperini, L., Polonia, A., Bortoluzzi, G., Henry, P., Le Pichon, X., Tryon, M., Çagatay, N., and Géli, L.: How far did the surface rupture of the 1999 Izmit earthquake reach in Sea of Marmara, Tectonics, 30, TC1010, doi:10.1029/2010TC002726, 2011.

Goda, K., Mori, N., Yasuda, T., Prasetyo, A., Muhammad, A. and Tsujio, D.: Cascading Geological Hazards and Risks of the 2018 Sulawesi Indonesia Earthquake and Sensitivity Analysis of Tsunami Inundation Simulations. Front. Earth Sci. 7:261. doi: 10.3389/feart.2019.00261, 2019.

Gundogdu, O.: Türkiye Depremlerinin Kaynak Parametreleri ve Aralarindaki Iliskiler (Source parameters of earthquakes in Turkey and their relationships), PhD Thesis, Istanbul University., p 120, 1986.

Hancilar, U.: Identification of elements at risk for a credible tsunami event for Istanbul, Natural Hazards & Earth System Sciences 12, 107-119, 2012.

Hanks, T.C. and H. Kanamori, 1979, "A Moment Magnitude Scale", Journal of Geophysical Research: Solid Earth, Volume 84, Issue B5, pages 2348–2350.

Hebert, H., Schindele, F., Altinok, Y., Alpar, B., and Gazioglu, C.: Tsunami hazard in the Marmara Sea (Turkey): a numerical approach to discuss active faulting and impact on the Istanbul coastal areas, Marine Geology, 215, 23–43, 2005.

Heidarzadeh, M., Muhari, A. and Wijanarto, A.B.: Insights on the Source of the 28 September 2018 Sulawesi Tsunami, Indonesia Based on Spectral Analyses and Numerical Simulations, Pure Appl. Geophys. 176, 25–43, https://doi.org/10.1007/s00024-018-2065-9, 2019.

Hergert, T. and Heidbach, O.: Slip-rate variability and distributed deformation in the Marmara Sea fault system, Nature Geoscience, 3, 2010.

Hergert, T., Heidbach, O., Becel, A., and Laigle, M.: Geomechanical model of the Marmara Sea region—I. 3-D contemporary kinematics, Geophys. J. Int., 185, 1073–1089, doi: 10.1111/j.1365-246X.2011.04991.x, 2011.

Imren, C., Le Pichon, X., Rangin, C., Demirbag, E., Ecevitoglu, B. and Gorur, N.: The North Anatolian Fault within the Sea of Marmara: a new interpretation based on multi-channel seismic and multi-beam bathymetry data, Earth and Planetary Science Letters 186, 143-158, 2001.

Jonkman, S. N., & Penning-Rowsell, E.: Human instability in Flood Fows. *J Am Water Resour As*., 2008.

Kaneko, F.: A Simulation Analysis of Possible Tsunami affecting the Istanbul Coast, Turkey, International Workshop on Tsunami Hazard Assessment and Management in Bangladesh, 2009.

Latcharote, P. Suppasri, A., Imamura, F., Aytore, B., and Yalciner, A. C.: Possible worst-case tsunami scenarios around the Marmara Sea from combined earthquake and landslide sources, Pure and Applied Geophysics, 173 (2), 3823-3846, 2016.

Le Pichon, X., Imren, C., Rangin, C., Sengor, A. M. C., and Siyako, M.: The South Marmara Fault, Int J Earth Sci (Geol Rundsch), 103, 219–231, doi: 10.1007/s00531-013-0950-0, 2014.

Le Pichon, X., Chamot-Rooke, N., Rangin, C, and Sengor, A. M. C.: The North Anatolian fault in the Sea of Marmara, Journal of Geophysical Research, 108, B4, 2179, doi:10.1029/2002JB001862, 2003.

Le Pichon, X., Sengor, A. M. C., Demirbag, E., Rangin, C., Imren, C., Armijo, R., Gorur, N., Cagatay, N., Mercier de Lepinay, B., Meyer, B., Saatcilar, R., and Tok, B.: The active Main Marmara Fault, Earth and Planetary Science Letters, 192, 595-616, 2001.

Lynett, P. J., Gately, K., Wilson, R., Montoya, L., Arcas, D., Aytore, B., and David, C. G.: Inter-model analysis of tsunami-induced coastal currents, Ocean Modelling, 114, 14-32, 2017.

Meade, B. J., Hager, B. H., McClusky, S. C., Reilinger, R. E., Ergintav, S., Lenk, O., Barka, A., and Ozener, H.: Estimates of seismic potential in the Marmara region from block models of secular deformation constrained by GPS measurements, Bull. Seismol. Soc. Am., 92, 208–215, 2002.

Mihailovic, J.: Memoir-Sur les Grands Tremblement de Terre de la Mer de Marmara, Beograd, 215–222, 1927.

Mikami, T., Shibayama, T., Esteban, M., Takabatake, T., Nakamura, R., Nishida,Y., Achiari, H. Rusli, Marzuki, A.G., Marzuki, M.F.H., Stolle, J., Krautwald, C., Robertson, I., Aranguiz, R. and Ohira, K.: Field Survey of the 2018 Sulawesi Tsunami: Inundation and Run-up Heights and Damage to Coastal Communities, Pure Appl. Geophys. 176, 3291–3304 Ó 2019 Springer Nature Switzerland AG https://doi.org/10.1007/s00024-019-02258-5, 2019.

Murru, M., A. Akinci, G. Falcone, S. Pucci, R. Console, and T. Parsons (2016), M ≥ 7 earthquake rupture forecast and time-dependent probability for the sea of Marmara region, Turkey, J. Geophys. Res. Solid Earth, 121, doi:10.1002/ 2015JB012595.

NAMI DANCE: Manual of Numerical Code NAMI DANCE, published in http://namidance.ce.metu.edu.tr, 2011.

Necmioglu, O.: Design and challenges for a tsunami early warning system in the Marmara Sea, Earth, Planets and Space, 68:13, doi: 10.1186/s40623-016-0388-2, 2016.

Necmioglu, O., and Ozel, N. M.: Earthquake Scenario-Based Tsunami Wave Heights in the Eastern Mediterranean and Connected Seas, Pure and Applied Geophysics, doi:10.1007/s00024-015-1069-y, 2015.

NTHMP: Proceedings and Results of the National Tsunami Hazard Mitigation Program 2015 Tsunami Current Modeling Workshop, 2015.

Oglesby, D. D. and Mai, P. M.: Fault geometry, rupture dynamics and ground motion from potential earthquakes on the North Anatolian Fault under the Sea of Marmara, Geophys. J. Int., 188, 1071–1087, doi: 10.1111/j.1365-246X.2011.05289.x, 2012.

Okada, Y.: Surface Deformation Due to Shear and Tensile Faults in a Half-Space, Bull. Seis. Soc. Am., 75, 4, 1135-1154, 1985.

Ozer Sozdinler, C., Yalciner, A.C., Zaytsev, A., Suppasri, A., Imamura, F.: Hydrodynamic Parameters in Kamaishi Bay during the 2011 Great East Japan Tsunami, J. of Pure Appl. Geophys., (DOI) 10.1007/s00024-015-1051-8, March 2015.

Oztin, F.: 10 Temmuz 1894 Istanbul Depremi Raporu, T.C. Bayindirlik ve Iskan Bakanligi, Afet Isleri Genel Mudurlugu, Deprem Arastırma Dairesi, (Report on 10 July 1894 Istanbul Earthquake by Ministry of Public Works and Settlement, General Directorate of Disaster Affairs, Department of Earthquake Research), Ankara, 1994.

Oztin, F. and Bayülke, N.: Historical earthquakes of Istanbul, Kayseri, Elazıg. In: Proceedings of the workshop on historical seismicity and seismotectonics of the Mediterranean region, 10–12 October 1990 (Istanbul), Turkish Atomic Energy Authority, Ankara, pp 150–173, 1991.

Özel, M. N., Necmioğlu, Ö., Yalçıner, A.C., Kalafat, D., Erdik, M.: Tsunami Hazard in the Eastern Mediterranean and its Connected Seas: Toward a Tsunami Warning Center in Turkey, Soil Dynamics and Earthquake Engineering, Volume 31, Issue 4, April 2011, Pages 598-610, 2011.

Pakoksung, K., Suppasri, A., Imamura, F., Athanasius, C., Omang, A., and Muhari, A.: Simulation of the submarine landslide tsunami on 28 September 2018 in Palu Bay, Sulawesi Island, Indonesia, using a two-layer model. Pure Appl. Geophys. 176, 3323–3350. doi: 10.1007/s00024-019-02235-y, 2019.

Reilinger, R., et al.: GPS constraints on continental deformation in the Africa-Arabia-Eurasia continental collision zone and implications for the dynamics of plate interactions, J. Geophys. Res. 111, B05411, doi:10.1029/2005JB004051, 2006.

Rothaus, R., Reinhardt, E., Noller, J.: Regional considerations of coastline change, tsunami damage and recovery along the southern coast of the Bay of Izmit (The Kocaeli (Turkey) earthquake of 17 August 1999). Nat Hazards 31:233–252, 2004.

Şengör, A. M. C., Grall, C., Imren, C., Le Pichon, X., Görür, N., Henry, P., Karabulut, H., and Siyako, M.: The geometry of the North Anatolian transform fault in the Sea of Marmara and its temporal evolution: implications for the development of intracontinental transform faults, Can. J. Earth Sci., 51, 222–242, dx.doi.org/10.1139/cjes-2013-0160, 2014

Şengör, A. M. C., Tuysuz, O., Imren, C., Sakınc, M., Eyidogan, H., Gorur, N., Le Pichon, X., and Rangin, C.: The North Anatolian fault: A new look, Annu. Rev. Earth Planet. Sci., 33, 37–112, 2005.

Takagi, H., Mikami, T., Fujii, D., Esteban, M., & Kurobe, S.: Mangrove forest against dyke-break-induced tsunami on rapidly subsiding coasts. *Natural Hazards and Earth System Sciences* 16(7) 1629-1638, 2016.

Tinti, S., Armigliato, A., Manucci, A., Pagnoni, G., Zaniboni, F., Yalciner, A. C., and Altinok, Y.: The generating mechanisms of the August 17, 1999 Izmit bay (Turkey) tsunami: Regional (tectonic) and local (mass instabilities) causes, Marine Geology 225, 311–330, 2006.

Ulrich, T., Vater, S., Madden, E.H. et al.: Coupled, physics-based modeling reveals earthquake displacements are critical to the 2018 Palu, Sulawesi Tsunami, Pure Appl. Geophys., 176: 4069. https://doi.org/10.1007/s00024-019-02290-5, 2019.

Utkucu, M., Kanbur, Z., Alptekin, O., and Sumbul, F.: Seismic behaviour of the North Anatolian Fault beneath the Sea of Marmara (NW Turkey): implications for earthquake recurrence times and future seismic hazard, Nat Hazards, 50, 45–71, doi:10.1007/s11069-008-9317-4, 2009.

Velioglu, D.: Advanced Two and Three Dimensional Tsunami Models: Benchmarking and Validation, Master's Thesis, Middle East Technical University, 2009.

Wells, D. L. and Coppersmith, K. J.: New empirical relationships among magnitude, rupture length, rupture width, rupture area, and surface displacement, Bulletin of the Seismological Society of America, 84, 4, 974-1002, 1994.

Yalciner, A.C., Alpar, B., Altinok, Y., Ozbay, I., Imamura, F.: Tsunamis in the Sea of Marmara; Historical documents for the past, models for the future, Marine Geology 190, 445-463, 2002.

Yolsal-Çevikbilen, S. and Taymaz, T.: Source Characteristics of the 28 September 2018 Mw 7.5 Palu-Sulawesi, Indonesia (SE Asia) Earthquake Based on Inversion of Teleseismic Bodywaves, Pure Appl. Geophys. 176, 4111–4126 Ó 2019 Springer Nature Switzerland AG https://doi.org/10.1007/s00024-019-02294-1, 2019.